Applied Physics Express **6** (2013) 052103
http://dx.doi.org/**10.7567/APEX.6.052103**

Dependence of Electron Overflow on Emission Wavelength and Crystallographic Orientation in Single-Quantum-Well III–Nitride Light-Emitting Diodes

Yoshinobu Kawaguchi[1,2], Shih-Chieh Huang[1,3], Robert M. Farrell[1], Yuji Zhao[4], James S. Speck[1], Steven P. DenBaars[1,4], and Shuji Nakamura[1,4]

[1]*Materials Department, University of California, Santa Barbara, CA 93106, U.S.A.*
[2]*Advanced Technology Research Laboratories, Sharp Corporation, Tenri, Nara 632-8567, Japan*
[3]*R&D Department of LED Unit, Walsin Lihwa Corporation, Taoyuan 326, Taiwan*
[4]*Electrical and Computer Engineering Department, University of California, Santa Barbara, CA 93106, U.S.A.*

Received February 20, 2013; accepted April 6, 2013; published online April 24, 2013

The dependence of electron overflow on peak emission wavelength was investigated in single-quantum-well (SQW) light-emitting diodes (LEDs) grown on the $(20\bar{2}1)$, $(20\bar{2}\bar{1})$, $(10\bar{1}0)$, and (0001) planes. Each plane exhibited a characteristic "critical" emission wavelength where the output power of LEDs (measured at a current density of 22 A/cm^2) without electron blocking layers (EBLs) decreased significantly compared with that of LEDs with EBLs. Compared with LEDs grown on the (0001) plane, LEDs grown on the $(20\bar{2}1)$, $(20\bar{2}\bar{1})$, and $(10\bar{1}0)$ planes exhibited shorter critical wavelengths, indicating that electron overflow was inhibited in LEDs grown on orientations with reduced polarization.

It is often assumed that electron blocking layers (EBLs) are an integral part of most III–nitride light-emitting diodes (LEDs) and laser diodes (LDs) because they are needed to prevent electron overflow.[1)] Many efforts have been made to improve the design of EBLs for (0001) Ga-polar LEDs because such modifications can have a significant impact on device performance metrics such as output power, voltage, characteristic temperature, and droop.[2–9)] Meanwhile, very interesting results have been reported recently regarding the use of EBLs for LEDs and LDs grown on other crystallographic orientations. Sizov et al. reported that semipolar LDs without EBLs exhibited a similar performance to semipolar LDs with EBLs.[10)] Likewise, Akyol et al. reported that $(000\bar{1})$ N-polar LEDs without EBLs exhibited relatively lower droop due to their higher potential barriers against carrier overflow than those of (0001) Ga-polar LEDs.[11)] According to these reports, the degree of electron overflow should depend on crystallographic orientation because of the differences in polarization direction and magnitude. In this work, we study the effect of EBLs on LED performance by using several different crystal planes to understand how polarization has an impact on electron overflow.

The samples used in this study were grown by metalorganic chemical vapor deposition (MOCVD). Free-standing GaN substrates were used for growing LEDs on the $(20\bar{2}1)$, $(20\bar{2}\bar{1})$, and $(10\bar{1}0)$ planes, which were supplied by Mitsubishi Chemical Corporation.[12)] Sapphire substrates were used for growing LEDs on the (0001) plane. The structure of the samples consisted of a 1 μm Si-doped n-GaN layer, a 20 nm undoped GaN barrier, an undoped InGaN single quantum well (SQW), a 25 nm undoped GaN barrier, a 35 nm Mg-doped p-AlGaN EBL, and a 120 nm Mg-doped p-GaN layer. The thickness of the quantum wells (QWs) was estimated to be 3 nm and the emission wavelength of the QWs was controlled by adjusting the growth temperature. The Al composition of the EBLs was changed by adjusting the trimethylaluminum (TMA) flow rate. The Al composition for a TMA flow rate of 1.15 sccm was estimated by X-ray diffraction (XRD) to be 14.9, 15.4, 15.3, and 14.5% on the $(20\bar{2}1)$, $(20\bar{2}\bar{1})$, $(10\bar{1}0)$, and (0001) planes, respectively. Following the MOCVD growth, the electrical and optical characteristics of the LEDs were measured by on-wafer probing of the devices under direct current (DC) conditions at 20 °C. Relative optical power was measured by back side emission through the substrates onto a calibrated broad-area Si photodiode. Based on previous experiments, we expect that the measured output powers for on-wafer probing would improve by a factor of 5–10 after device packaging.

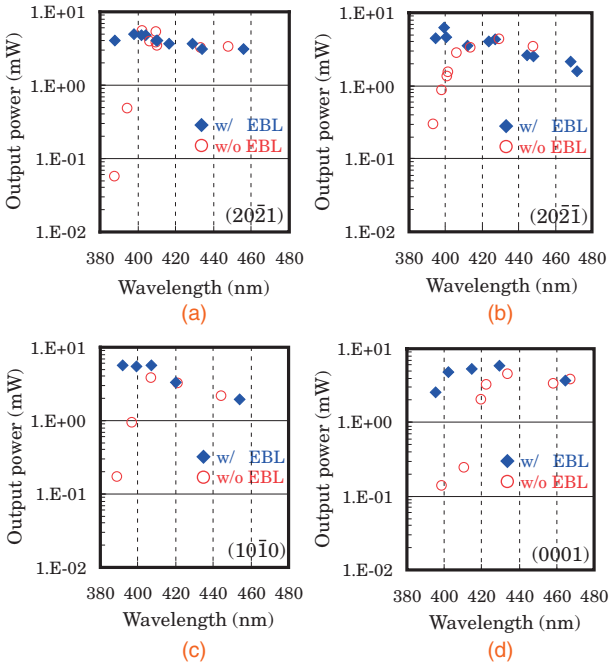

Fig. 1. Dependence of output power on peak emission wavelength for LEDs with and without EBLs on the (a) $(20\bar{2}1)$, (b) $(20\bar{2}\bar{1})$, (c) $(10\bar{1}0)$, and (d) (0001) planes.

Figure 1 shows the peak emission wavelength dependence of output power of the LEDs with EBLs (with TMA flow rates of 1.15 sccm) and LEDs without EBLs on the $(20\bar{2}1)$, $(20\bar{2}\bar{1})$, $(10\bar{1}0)$, and (0001) planes. All output power measurements were taken at a current (current density) of 20 mA (22 A/cm^2). Each plane exhibited a characteristic "critical" emission wavelength where the output power of LEDs without EBLs decreased significantly compared with that of LEDs with EBLs. Except for the (0001) plane, no difference was seen between LEDs with and without EBLs for wavelengths longer than 420 nm. This result indicates that the reduced polariza-

tion by the use of the semipolar $(20\bar{2}1)$ and $(20\bar{2}\bar{1})$ planes or the nonpolar $(10\bar{1}0)$ plane is effective for suppressing electron overflow at longer wavelengths when the active region consists of a SQW. The significant decrease in the output power of LEDs without EBLs at wavelengths shorter than the critical wavelength, which is observed on all planes, is interpreted as being due to electron overflow from shallow QWs with low In fractions. Interestingly, even the (0001) plane did not show any difference in output power between LEDs with and without EBLs in the blue region of the spectrum where many studies have shown the necessity for an EBL.[2–7] Although we suspect that this may be because the active region used in this study is a SQW instead of a multiple quantum well (MQW), which is the structure used for most of blue LEDs, the effect of the number of QWs on electron overflow is unknown and is still under investigation.

Next, we investigated the impact of polarization direction on electron overflow. Polarization in the direction of the N-polar *c*-plane, or the $(000\bar{1})$ plane, acts to suppress electron overflow, while that of the Ga-polar *c*-plane, or the (0001) plane, acts to enhance electron overflow.[11,13,14] This means that in addition to the magnitude of polarization, its direction can also have an impact on electron overflow. The $(20\bar{2}1)$ and $(20\bar{2}\bar{1})$ planes have opposite directions of polarization while their magnitudes are equal.[15,16] As discussed by Feezell et al.,[17] the $(20\bar{2}1)$ plane has the same polarization direction as the $(000\bar{1})$ plane, while the $(20\bar{2}\bar{1})$ plane has the same polarization direction as the (0001) plane. Thus, the $(20\bar{2}1)$ plane is expected to exhibit less electron overflow than the $(20\bar{2}\bar{1})$ plane. To test this hypothesis, the output power was compared for LEDs grown on the $(20\bar{2}1)$ and $(20\bar{2}\bar{1})$ planes with different TMA flow rates in their EBLs and different emission wavelengths. The dependence of output power on TMA flow rate is presented in Fig. 2 for LEDs with peak emission wavelengths of 390, 400, 410, and 430 nm. The variation in each wavelength was less than 5 nm. For an emission wavelength of 390 nm, the LEDs grown on both the $(20\bar{2}1)$ and $(20\bar{2}\bar{1})$ planes showed a significant decrease in output power as the TMA flow rate was decreased. Although both planes showed a significant decrease in output power with decreasing TMA flow rate, the output power of LEDs grown on the $(20\bar{2}1)$ plane was slightly lower than the output power of LEDs grown on $(20\bar{2}\bar{1})$ plane. Since the output power of LEDs without sufficient EBLs was shown to be highly sensitive to the emission wavelength below the critical wavelength (see Fig. 1), this difference in output power was probably caused by small differences in the emission wavelength between the two sets of samples. Nevertheless, the 390 nm LEDs grown on the $(20\bar{2}1)$ and $(20\bar{2}\bar{1})$ planes behaved similarly by showing a significant decrease in output power with decreasing TMA flow rate. In contrast, for emission wavelengths of 410 and 430 nm, the output power did not depend on Al composition for LEDs grown on both the $(20\bar{2}1)$ and $(20\bar{2}\bar{1})$ planes. However, a clear difference was seen between the LEDs grown on the $(20\bar{2}1)$ and $(20\bar{2}\bar{1})$ planes for a peak emission wavelength of 400 nm, with LEDs grown on the $(20\bar{2}1)$ plane maintaining higher output powers at low TMA flow rates than LEDs grown on the $(20\bar{2}\bar{1})$ plane. In summary, LEDs grown on the $(20\bar{2}1)$ plane maintained a constant output power to a shorter emission wavelength than LEDs grown on the $(20\bar{2}\bar{1})$ plane. This result confirms our hypothesis that the $(20\bar{2}1)$ plane exhibits less electron overflow than the $(20\bar{2}\bar{1})$ plane due to the favorable direction of the polarity to suppress electron overflow.

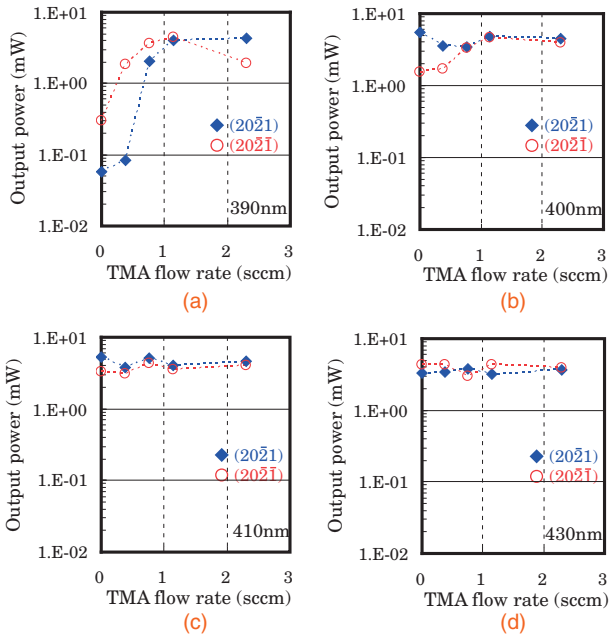

Fig. 2. Dependence of output power on TMA flow rate for LEDs on the $(20\bar{2}1)$ and $(20\bar{2}\bar{1})$ planes with peak emission wavelengths of (a) 390, (b) 400, (c) 410, and (d) 430 nm.

To verify the above discussion about the relationship between the polarization and the probability of electron overflow, energy band diagrams were calculated using the SiLENSe version 5.2 software package.[18] Figure 3 shows the calculated conduction band diagrams and electron ground state wavefunction energy levels for LEDs with EBLs on the $(20\bar{2}\bar{1})$, $(20\bar{2}1)$, $(10\bar{1}0)$, and (0001) planes at a current density of 22 A/cm^2. The In fraction in each QW was tuned to obtain a peak emission wavelength of 400 nm for each plane. As shown in Fig. 3, the potential energy barrier for electron escape in each QW (the energy difference between the electron ground state wavefunction energy levels and the quantum barrier) was extracted to estimate the probability for electron overflow. The $(20\bar{2}1)$ plane had the largest potential energy barrier (0.29 eV), the $(10\bar{1}0)$ plane had the second largest potential energy barrier (0.23 eV), the $(20\bar{2}\bar{1})$ plane had the third largest potential energy barrier (0.18 eV), and the (0001) plane had the smallest potential energy barrier (0.08 eV) among the four planes. These values for the potential energy barrier are consistent with the critical wavelengths obtained experimentally and shown in Fig. 1. Although the (0001) plane has a smaller In fraction (~10.5%) than the other planes (~12%), we point out that the In fraction is not a major factor in the variations in the potential energy barrier because the difference in the QW-to-barrier conduction band offset is only 0.04 eV between the (0001) plane and the other planes. Rather, it is the large polarization of the (0001) plane that makes the potential energy barrier lower than those of the other planes. Likewise, the comparison between the $(20\bar{2}1)$ and $(20\bar{2}\bar{1})$ planes in Figs. 2 and 3 also indicates that the direction of the polarization has an impact on the potential barrier. Thus, the simulation results verify our interpretation of the experimental results in this study.

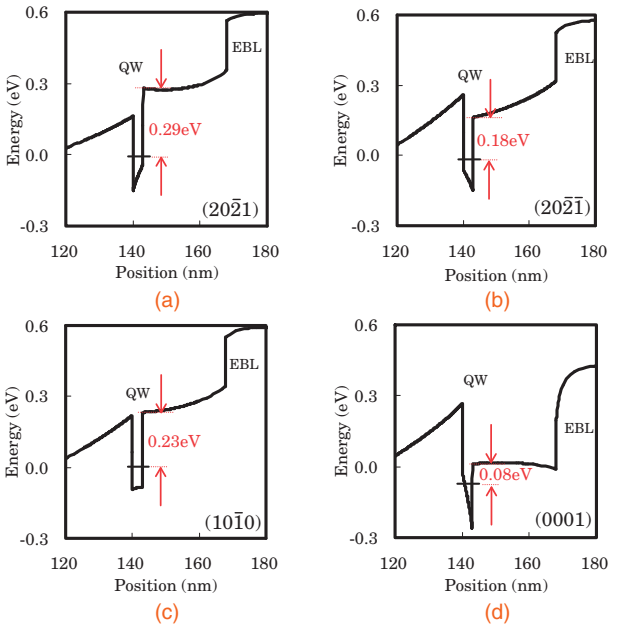

Fig. 3. Calculated conduction band diagrams and electron ground state wavefunction energy levels for LEDs with EBLs on the (a) (20$\bar{2}$1), (b) (20$\bar{2}\bar{1}$), (c) (10$\bar{1}$0), and (d) (0001) planes at a current density of 22 A/cm^2. The energy difference between the electron ground state wavefunction energy levels and the quantum barrier is shown in the figures.

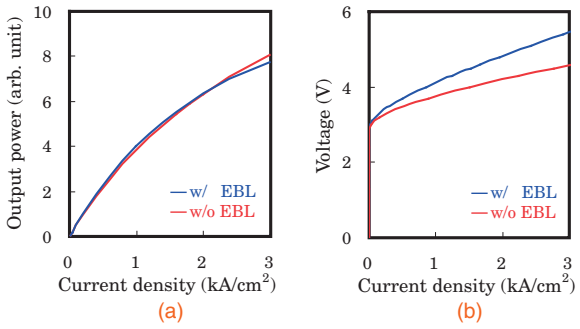

Fig. 4. (a) Output power and (b) forward voltage of LEDs with and without EBLs as a function of DC forward current. These LEDs were grown on the (20$\bar{2}$1) plane and had a peak emission wavelength of 400 nm.

Finally, output power was compared at high current densities to assess the effect of high levels of carrier injection on electron leakage. Figures 4(a) and 4(b) show the output power and forward voltage, respectively, of LEDs with EBLs (with a TMA flow rate of 1.15 sccm) and without EBLs as a function of DC forward current. These LEDs were grown on the (20$\bar{2}$1) plane and had a peak emission wavelength of 400 nm, corresponding to the wavelength region in Fig. 1(a) where there was no significant difference in output power between LEDs with and without EBLs. Small p-contacts consisting of Pd/Au circles with a radius of 40 μm were used for this measurement to obtain high current densities. As shown in Fig. 4(a), the output power was nearly identical for LEDs with and without EBLs, even at current densities as high as 3 kA/cm^2. In contrast, as depicted in Fig. 4(b), the forward voltage of the LED with an EBL was significantly larger than that of the LED without an EBL, especially at high current densities. Although further investigation is necessary, these results indicate that the increased voltage in the LED with EBL may be due to the high resistance of the p-AlGaN layer.[19,20] These results also indicate that an EBL-free (20$\bar{2}$1) LED structure could provide the benefit of a low forward voltage without a loss in output power compared with a conventional (20$\bar{2}$1) LED structure with an EBL.

In conclusion, we investigated the dependence of electron overflow on peak emission wavelength in SQW LEDs grown on the (20$\bar{2}$1), (20$\bar{2}\bar{1}$), (10$\bar{1}$0), and (0001) planes. Compared with the (0001) plane, the (20$\bar{2}$1), (20$\bar{2}\bar{1}$), and (10$\bar{1}$0) planes exhibited shorter critical emission wavelengths where the output power of LEDs without EBLs decreased significantly compared with that of LEDs with EBLs. These results indicate that reduced polarization is effective for suppressing electron overflow. In addition, the (20$\bar{2}$1) plane, which has a polarization in the same sense as the (000$\bar{1}$) N-polar plane, exhibited a shorter critical wavelength than the (20$\bar{2}\bar{1}$) plane, which has a polarization in the same sense as the (0001) Ga-polar plane. These observations indicate that planes with polarization in the same sense as the (000$\bar{1}$) N-polar plane are favorable for suppressing electron overflow.

Acknowledgments The authors would like to thank Mitsubishi Chemical Corporation for supplying the freestanding GaN substrates used in this study. This was work was supported by the Solid State Lighting and Energy Center (SSLEC) at UCSB. A portion of this work was performed in the UCSB nanofabrication facility, part of the NSF NNIN network (ECS-0335765), as well as the UCSB MRL, which is supported by the NSF MRSEC program (DMR-1121053).

1) E. F. Schubert: *Light-Emitting Diodes* (Cambridge University Press, Cambridge, U.K., 2006) 2nd ed., pp. 81–83.
2) M.-H. Kim, M. F. Schubert, Q. Dai, J. K. Kim, E. F. Schubert, J. Piprek, and Y. Park: Appl. Phys. Lett. **91** (2007) 183507.
3) Y.-K. Kuo, J.-Y. Chang, and M.-C. Tsai: Opt. Lett. **35** (2010) 3285.
4) C. H. Wang, C. C. Ke, C. Y. Lee, S. P. Chang, W. T. Chang, J. C. Li, Z. Y. Li, H. C. Yang, H. C. Kuo, T. C. Lu, and S. C. Wang: Appl. Phys. Lett. **97** (2010) 261103.
5) S. Choi, M.-H. Ji, J. Kim, H. J. Kim, M. M. Satter, P. D. Yoder, J.-H. Ryou, R. D. Dupuis, A. M. Fischer, and F. A. Ponce: Appl. Phys. Lett. **101** (2012) 161110.
6) Y.-Y. Zhang and G.-R. Yao: J. Appl. Phys. **110** (2011) 093104.
7) Z. Liu, J. Ma, X. Yi, E. Guo, L. Wang, J. Wang, N. Lu, J. Li, I. Ferguson, and A. Melton: Appl. Phys. Lett. **101** (2012) 261106.
8) J. Zhang, Y. Sakai, and T. Egawa: IEEE J. Quantum Electron. **46** (2010) 1854.
9) H. Hirayama, Y. Tsukada, T. Maeda, and N. Kamata: Appl. Phys. Express **3** (2010) 031002.
10) D. Sizov, R. Bhat, K. Song, D. Allen, B. Paddock, S. Coleman, L. C. Hughes, and C. Zah: Appl. Phys. Express **4** (2011) 102103.
11) F. Akyol, D. N. Nath, S. Krishnamoorthy, P. S. Park, and S. Rajan: Appl. Phys. Lett. **100** (2012) 111118.
12) K. Fujito, K. Kiyomi, T. Mochizuki, H. Oota, H. Namita, S. Nagao, and I. Fujimura: Phys. Status Solidi A **205** (2008) 1056.
13) S.-H. Yen and Y.-K. Kuo: J. Appl. Phys. **103** (2008) 103115.
14) A. Konar, A. Verma, T. Fang, P. Zhao, R. Jana, and D. Jena: Semicond. Sci. Technol. **27** (2012) 024018.
15) Y. Kawaguchi, C. Y. Huang, Y. R. Wu, Q. Yan, C. C. Pan, Y. Zhao, S. Tanaka, K. Fujito, D. Feezell, C. G. V. de Walle, S. P. DenBaars, and S. Nakamura: Appl. Phys. Lett. **100** (2012) 231110.
16) Y. Kawaguchi, C. Y. Huang, Y. R. Wu, Y. Zhao, S. P. DenBaars, and S. Nakamura: to be published in Jpn. J. Appl. Phys.
17) D. F. Feezell, J. S. Speck, S. P. DenBaars, and S. Nakamura: J. Disp. Technol. **9** (2013) 190.
18) V. F. Mymrin, K. A. Bulashevich, N. I. Podolskaya, I. A. Zhmakin, S. Y. Karpov, and Y. N. Makarov: Phys. Status Solidi C **2** (2005) 2928.
19) M. Suzuki, J. Nishio, M. Onomura, and C. Hongo: J. Cryst. Growth **189–190** (1998) 511.
20) S.-N. Lee, J. Son, T. Sakong, W. Lee, H. Paek, E. Yoon, J. Kim, Y.-H. Cho, O. Nam, and Y. Park: J. Cryst. Growth **272** (2004) 455.